

1 **Supplemental Material:**

2 **The temperature dependence of phonons in FeGe<sub>2</sub>**

3 Hillary L. Smith,<sup>1,\*</sup> Yang Shen,<sup>1,\*</sup> Dennis S. Kim,<sup>1</sup> Fred C. Yang,<sup>1</sup> C.P.  
4 Adams,<sup>2</sup> Chen W. Li,<sup>3</sup> D.L. Abernathy,<sup>4</sup> M.B. Stone,<sup>4</sup> and B. Fultz<sup>1</sup>

5 <sup>1</sup>*California Institute of Technology,*

6 *Department of Applied Physics and Materials*

7 *Science, Pasadena, California 91125, USA<sup>†</sup>*

8 <sup>2</sup>*St. Francis Xavier University, Department of Physics,*

9 *Antigonish, NS, Canada B2G 2W5*

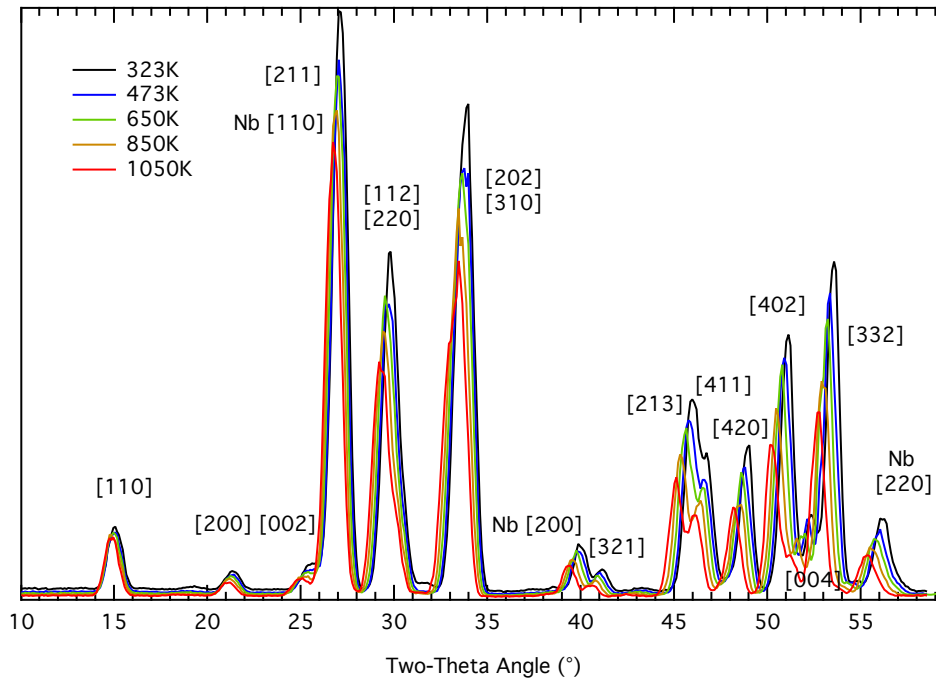
10 <sup>3</sup>*University of California Riverside,*

11 *Department of Mechanical Engineering, Riverside, California 92521, USA*

12 <sup>4</sup>*Quantum Condensed Matter Division,*

13 *Oak Ridge National Laboratory, Oak Ridge, Tennessee 37831, USA*

14 (Dated: August 5, 2018)



1

2 **FIG. 1. Neutron powder diffraction patterns of polycrystalline FeGe<sub>2</sub> at 323, 476, 650,**  
 3 **850 and 1050 K.** Diffraction patterns were obtained from elastic scattering in the experimental  
 4 data sets containing the inelastic neutron scattering measurements used for the phonon densities of  
 5 states. Intensity is plotted as a function of  $Q$ , with each colored curve corresponding to a different  
 6 temperature. The [hkl] index of each peak is labeled. Three peaks from the Nb sample holder are  
 7 indexed.

---

8 \* These two authors contributed equally

9 † HLS@caltech.edu

10 <sup>1</sup> E. Havinga, H. Damsma, and P. Hokkeling, Journal of the Less Common Metals **27**, 169 (1972).

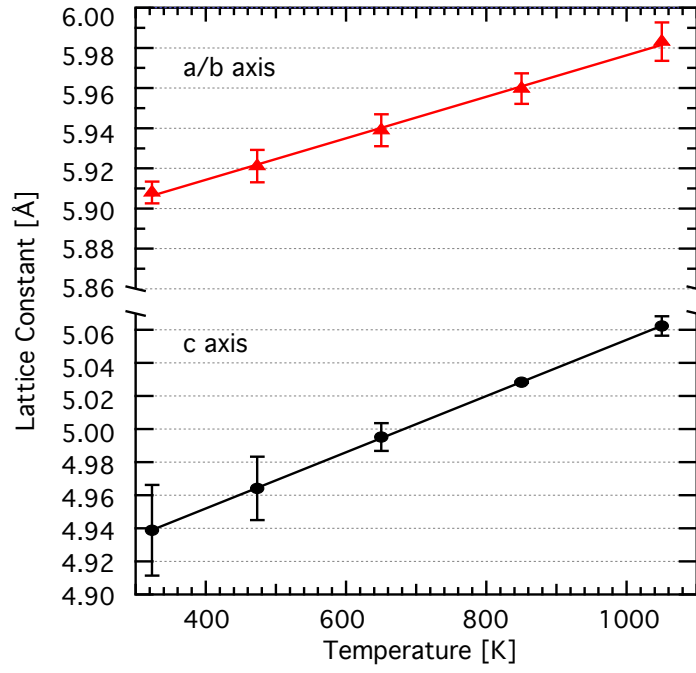


FIG. 2. **Lattice constants of FeGe<sub>2</sub>**. The lattice constants for  $a = b > c$  are shown as functions of temperature. A linear thermal expansion of the lattice constants is observed, in agreement with previously reported room temperature data<sup>1</sup>.

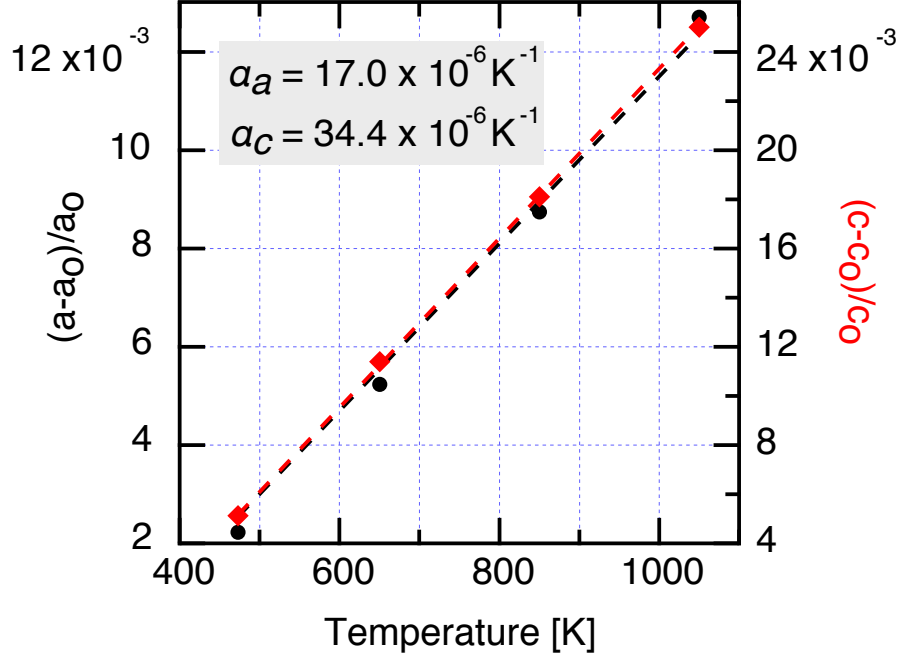
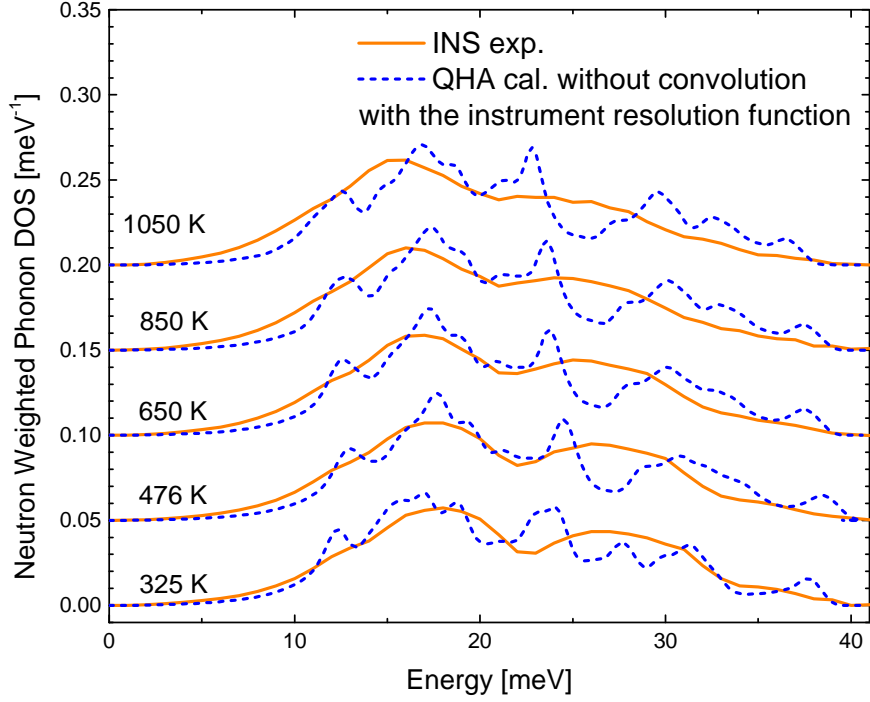


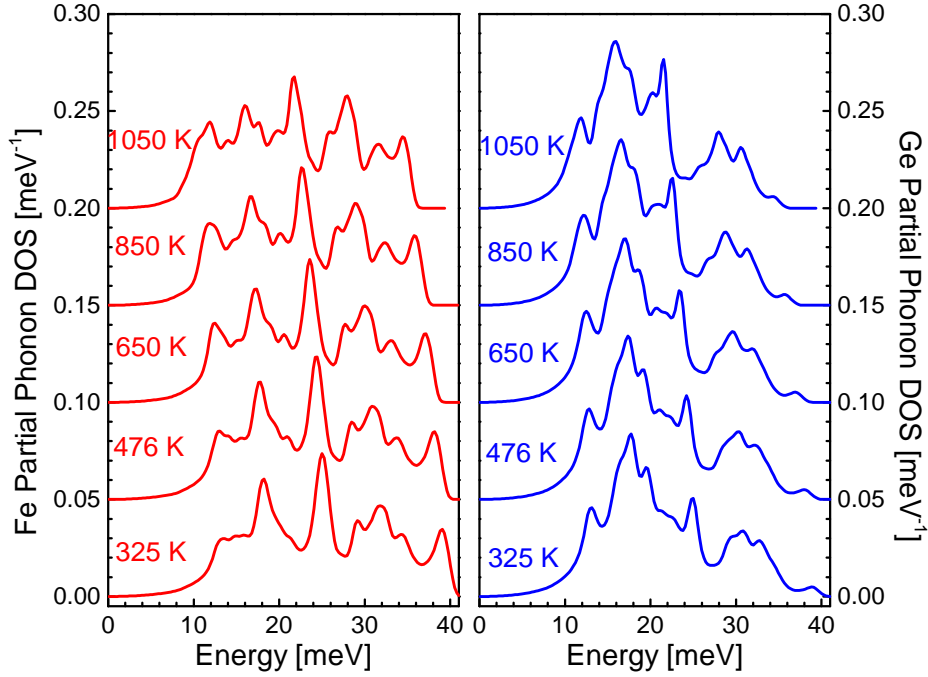
FIG. 3. **Thermal Expansion of FeGe<sub>2</sub>**. The coefficient of thermal expansion is obtained by fitting the data in Fig. 2 to

$$\frac{a_T - a_o}{a_o} = \alpha_a \cdot (T - T_o) \quad (2)$$

where  $a_o$  represents the lattice parameter at  $T = T_o$  ( $T_o=323$  K) and  $\alpha_a$  is the linear thermal expansion coefficient of the lattice parameter in the  $a$  direction. This is a first order temperature independent approximation of the thermal expansion coefficient. The linear thermal expansion in the  $c$  direction is found by application of the same equation with  $a$  replaced by  $c$ .



(a)



(b)

FIG. 4. **Detailed computational results with quasiharmonic approximation.** (a) Calculated phonon DOS (dash line) without convolution with the instrument resolution function. Experimental data from INS (solid line) is also presented for comparison. (b) Calculated Fe (left panel, in red) and Ge (right panel, in blue) partial phonon DOS. Curves are normalized to unity and offset for clarity.

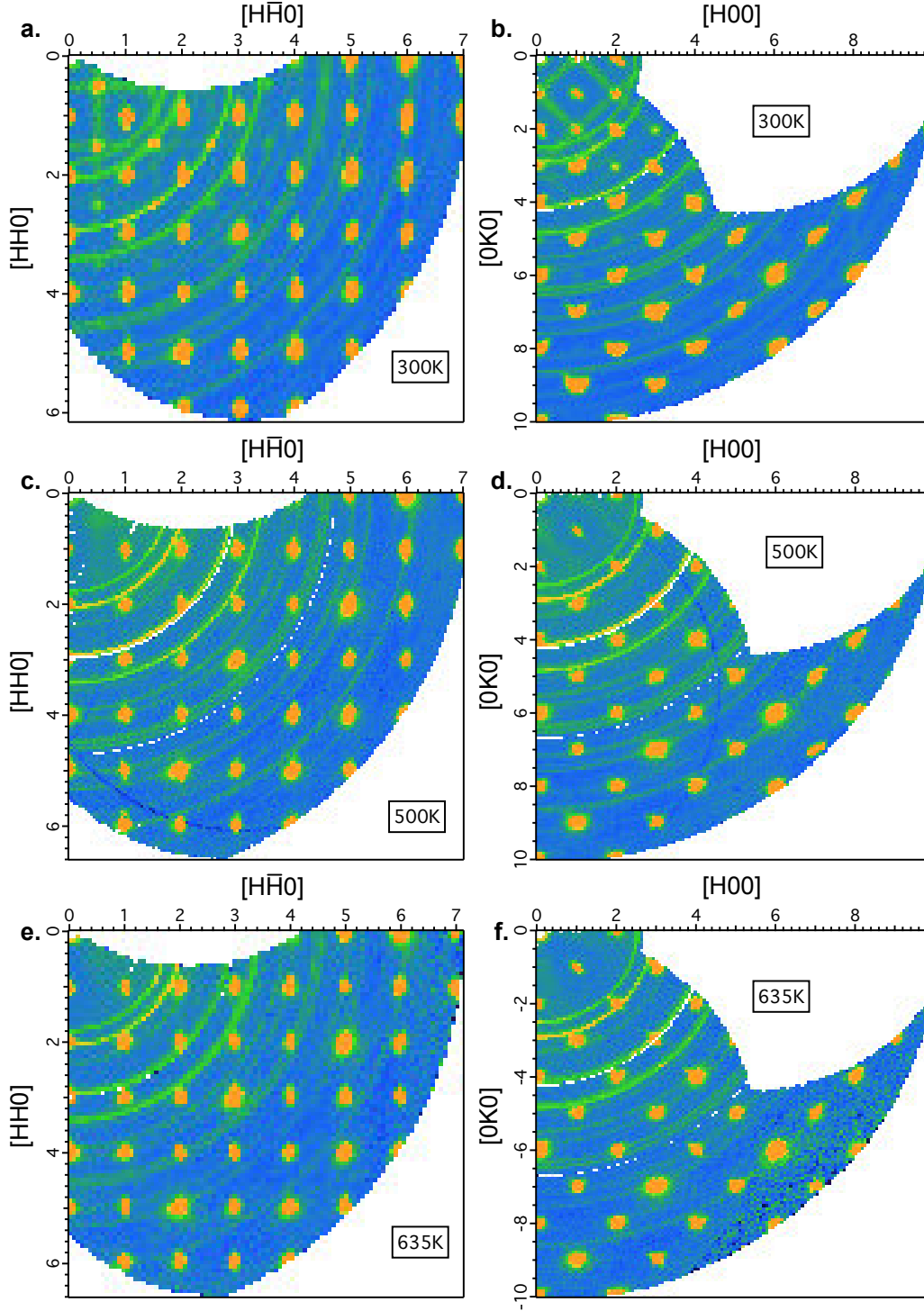


FIG. 5. **Elastic scattering from single crystal FeGe<sub>2</sub>.** The crystal was oriented in the [00L] zone axis, with the [HK0] crystallographic plane horizontal. Slices of the elastic plane were obtained by integrating from -1 to 1 meV in energy, and over the L-direction from -0.15 to 0.15. For the tetragonal symmetry of the crystal, the [0K0] and [H00] directions are crystallographically equivalent, as are the [HH0] and [H $\bar{H}$ 0] directions. (a) and (b) 300 K, (c) and (d) 500 K (e) and (f) 635 K.

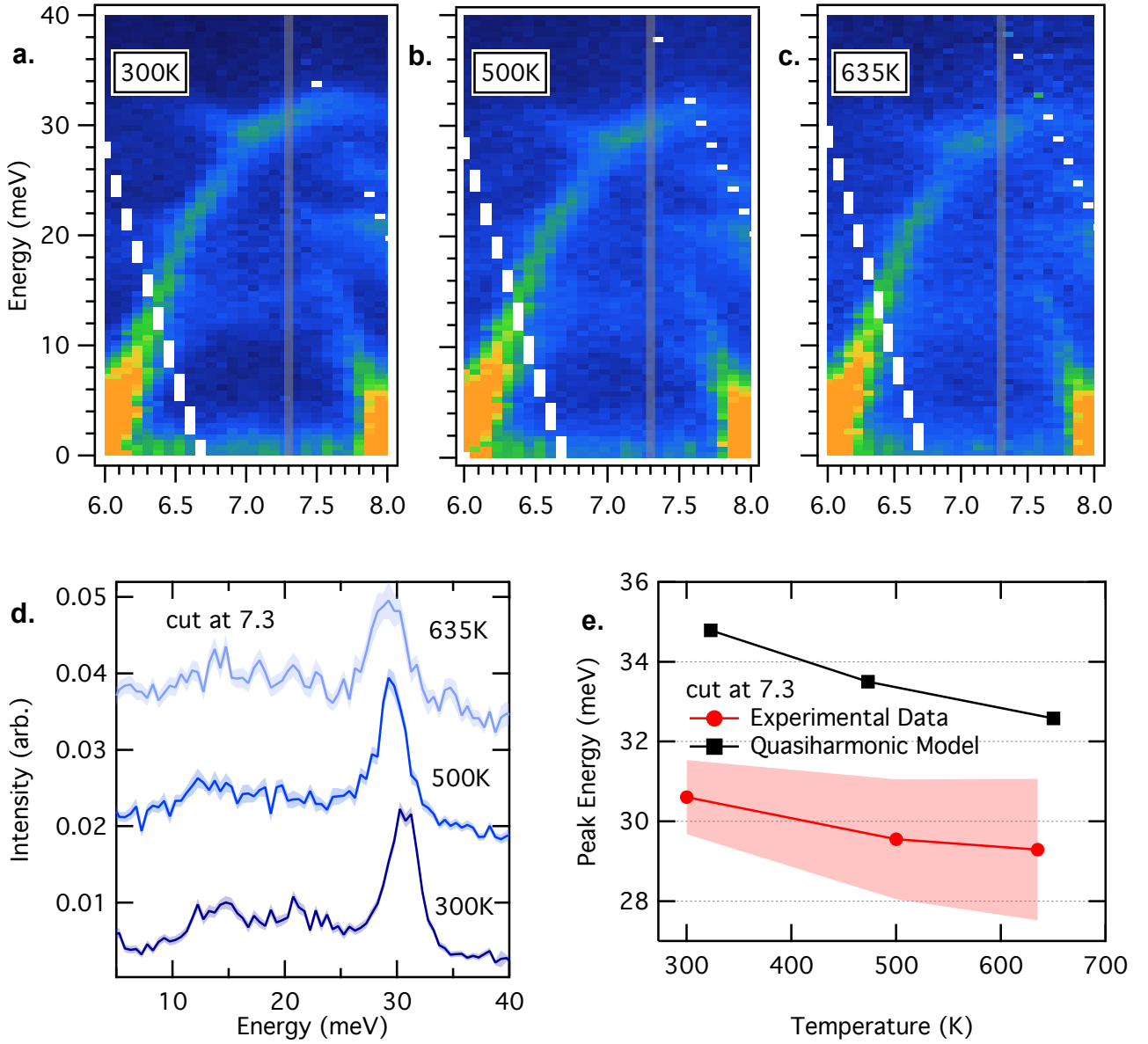


FIG. 6. Inelastic scattering from single crystal FeGe<sub>2</sub> along the [0K0] direction. (a)-(c) The [0K0] direction at 300, 500, and 635 K, respectively. The gray stripe shows the region of the cut shown in panel (d). (d) Cut of data at 7.3 r.l.u. is shown for 300 K (dark blue), 500 K (blue), and 635 K (light blue), offset for clarity, with error bars shown by the width of the curve. (e) Centers of the high-energy modes from fits to the experimental data in panel (d) are in red, with the shaded region showing the peak FWHM. The center of the high-energy mode predicted by the quasiharmonic model is shown in black.

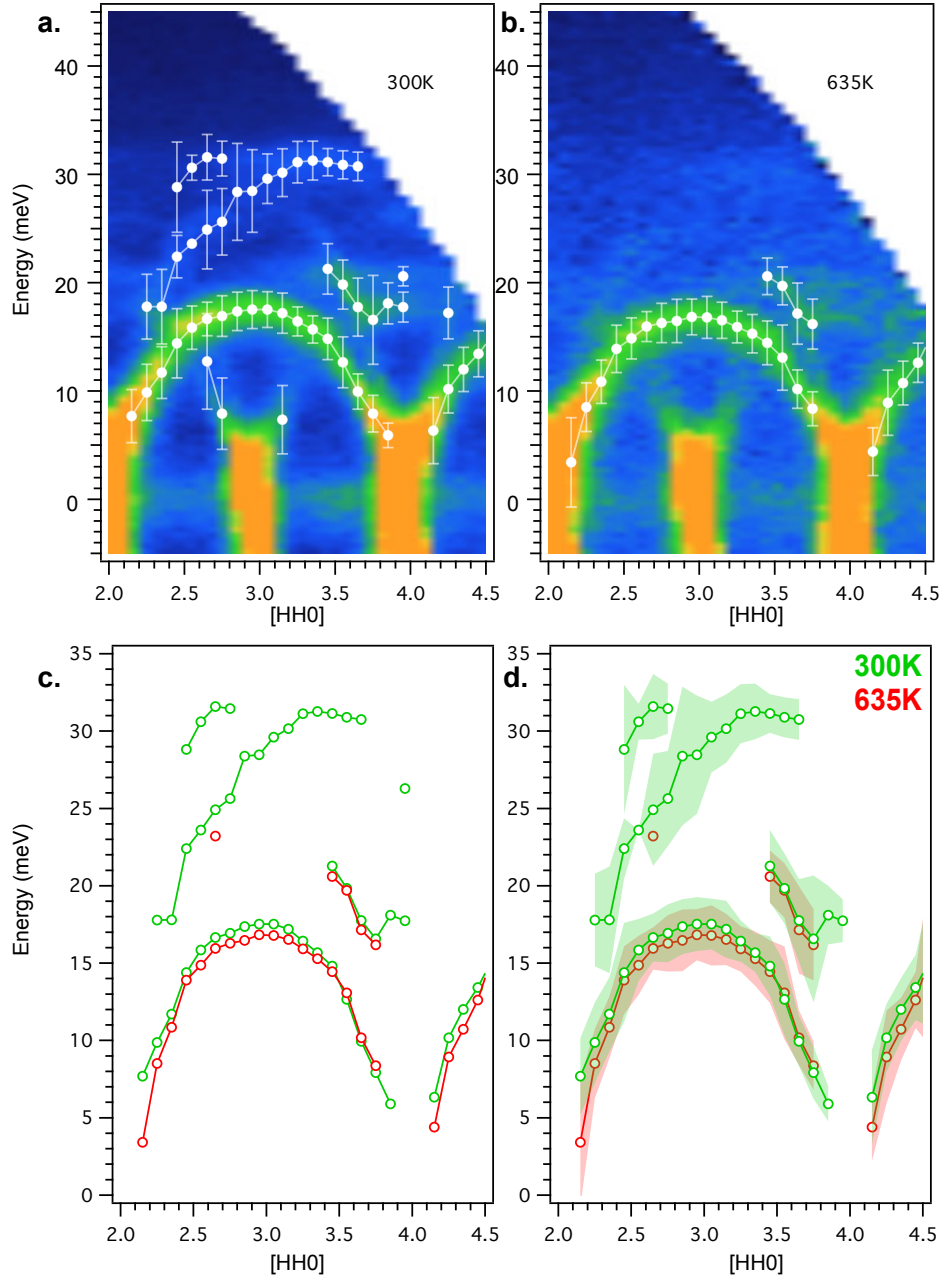


FIG. 7. Inelastic scattering from single crystal FeGe<sub>2</sub> along the [HH0] direction. (a) and (b) The [HH0] direction at 300 and 635 K with the positions of the peaks indicated by white circles and bars showing the FWHM from the fits. (c) The peak centers at 300 and 635 K, showing thermal shifts of the dispersions. (d) The same peak centers in (c), but with shaded regions indicating the FWHM, showing approximately the change in thermal broadening with temperature.

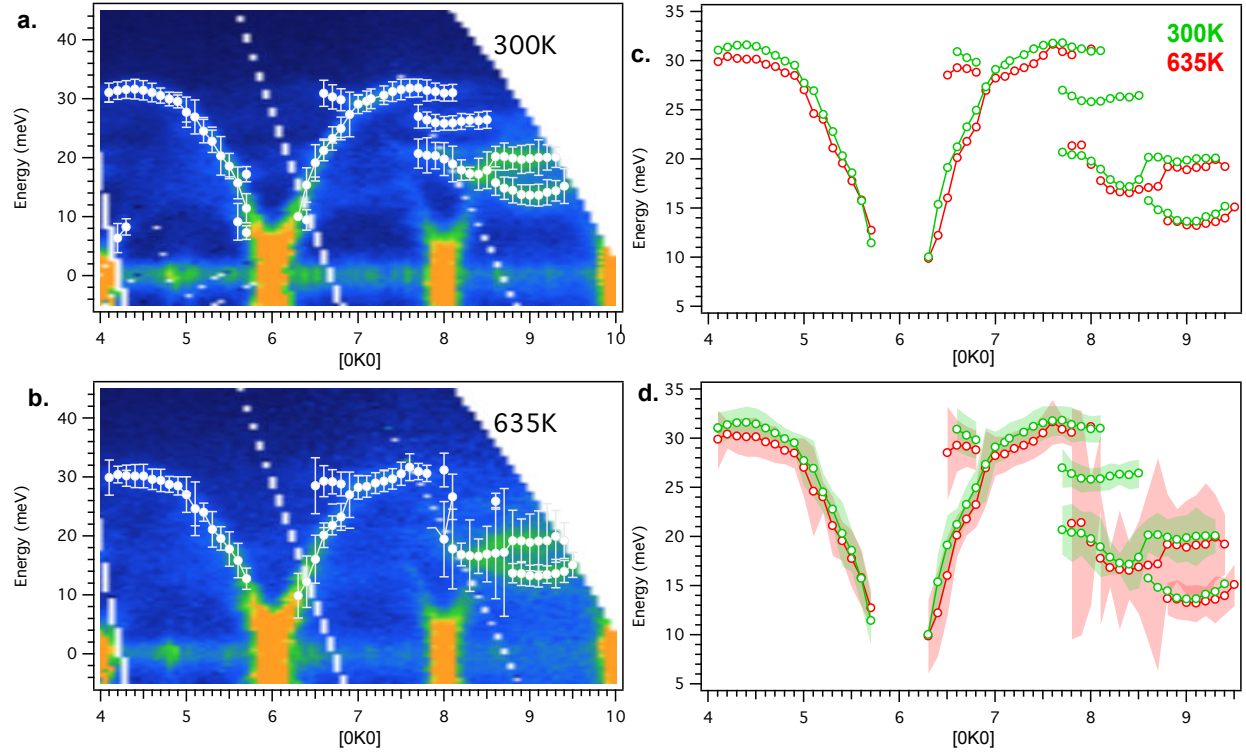


FIG. 8. **Inelastic scattering from single crystal FeGe<sub>2</sub> along the [0K0] direction.** (a) and (b) The [0K0] direction at 300 and 635 K, with peak centers indicated with white circles, and bars showing the FWHM obtained from the fits. (c) The peak centers at 300 and 635 K, showing thermal shifts of the dispersions. (d) The same peak centers in (c), but with shaded regions indicating the FWHM, showing approximately the change in thermal broadening with temperature.

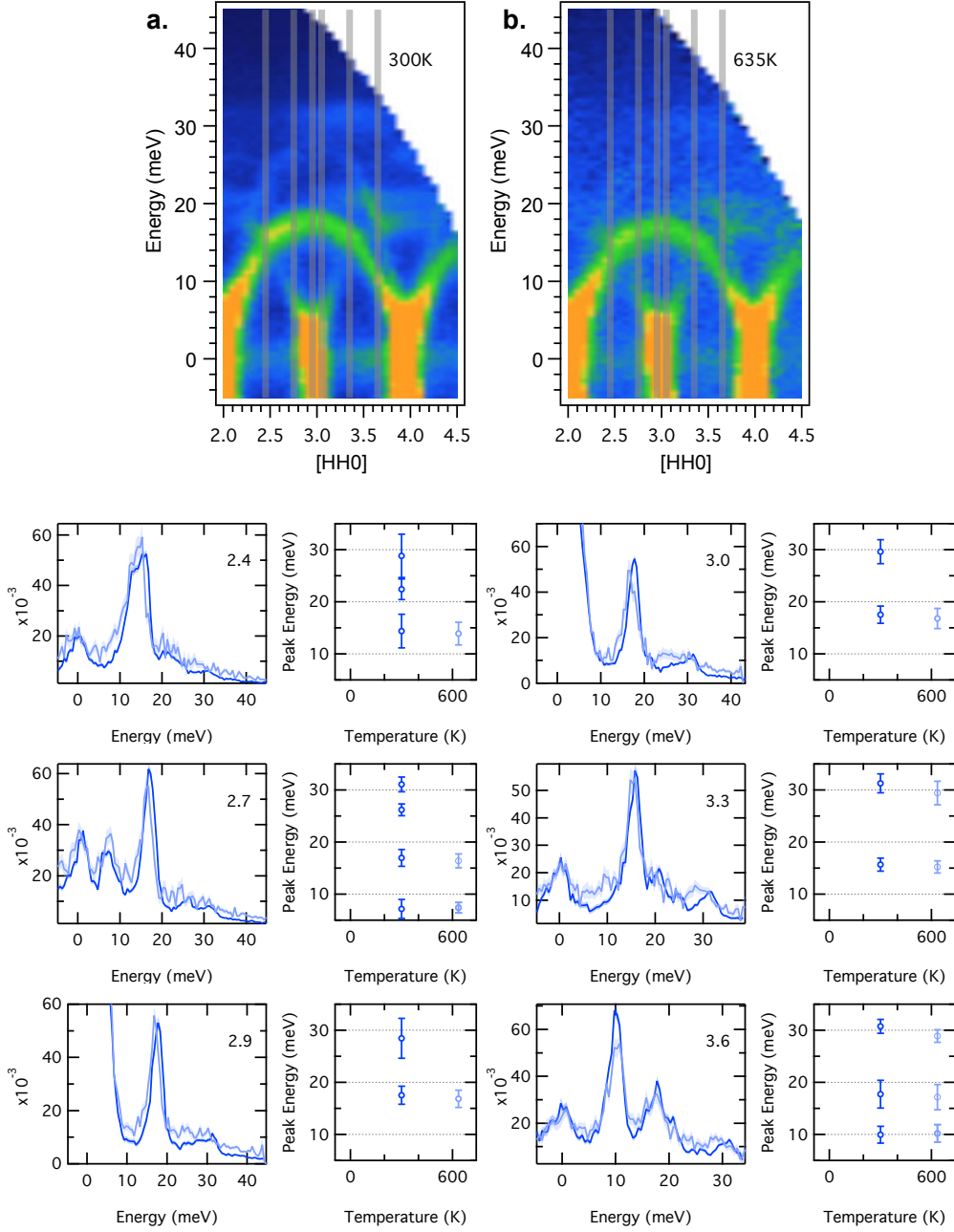


FIG. 9. Inelastic scattering from single crystal  $\text{FeGe}_2$  along the  $[\text{HH}0]$  direction. (a) and (b) The  $[\text{HH}0]$  dispersions at 300 and 635 K. The gray stripes indicate the regions of the cuts below. Cuts of data at the r.l.u. indicated on the plots are shown for 300 K (dark blue) and 635 K (light blue). To the right of each plot are shown centers of the peaks (identified in corresponding color), with bars showing the FWHM of the peaks.

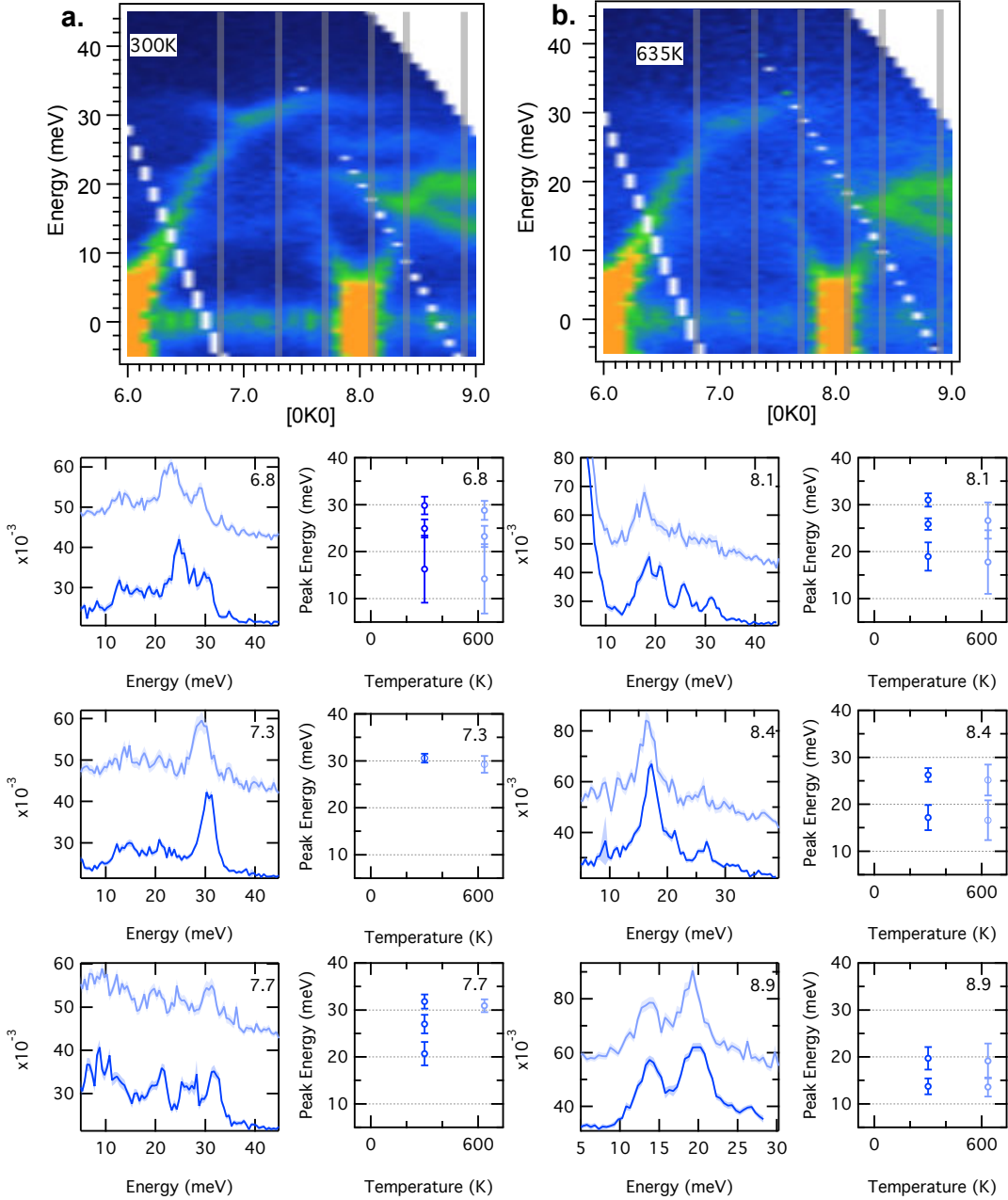


FIG. 10. Inelastic scattering from single crystal  $\text{FeGe}_2$  along the  $[0K0]$  direction. (a) and (b) The  $[0K0]$  dispersions at 300 and 635 K. The gray stripes indicate the regions of the cuts below. Cuts of data at the r.l.u. indicated on the plots are shown for 300 K (dark blue) and 635 K (light blue). To the right of each plot are shown centers of the peaks (identified in corresponding color), with bars showing the FWHM of the peaks.

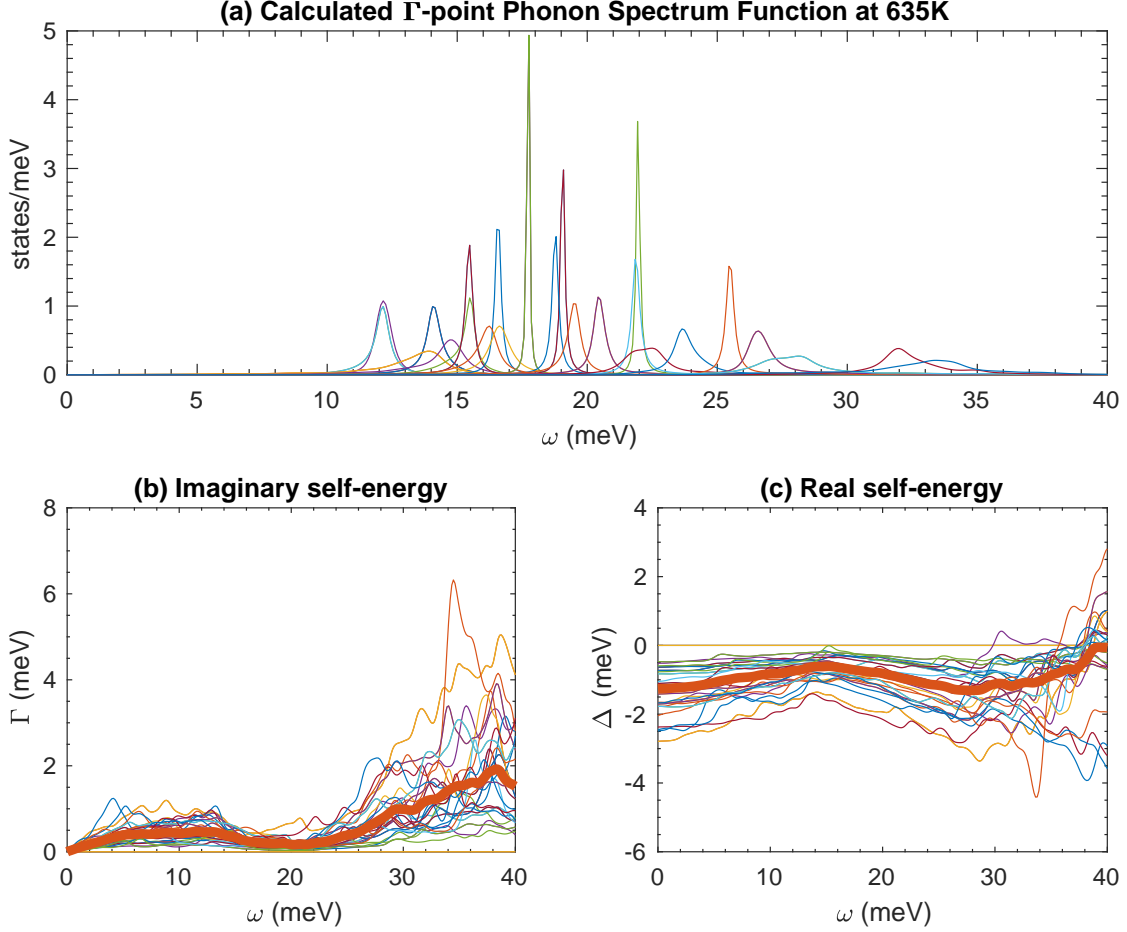


FIG. 11. Calculated phonon self-energy of  $\Gamma$ -point phonons in  $\text{FeGe}_2$  at 635 K. (a) The phonon spectrum at  $\Gamma$  at 635 K was calculated by *ab initio* stochastically initialized temperature-dependent effective potential method (s-TDEP) method. Colors represent different phonon branches. (b, c) Third-order force constants were used to calculate the imaginary part and the real part of the phonon self-energy. The averaged values are shown by the bold red line. This is consistent with the results in our main text obtained from the phonon DOS measurements and single crystal data. And it shows that QHA is not enough, because the cubic anharmonicity plays an important role in the phonon broadening in the high-energy modes of  $\text{FeGe}_2$ . More results are shown in the next figure.

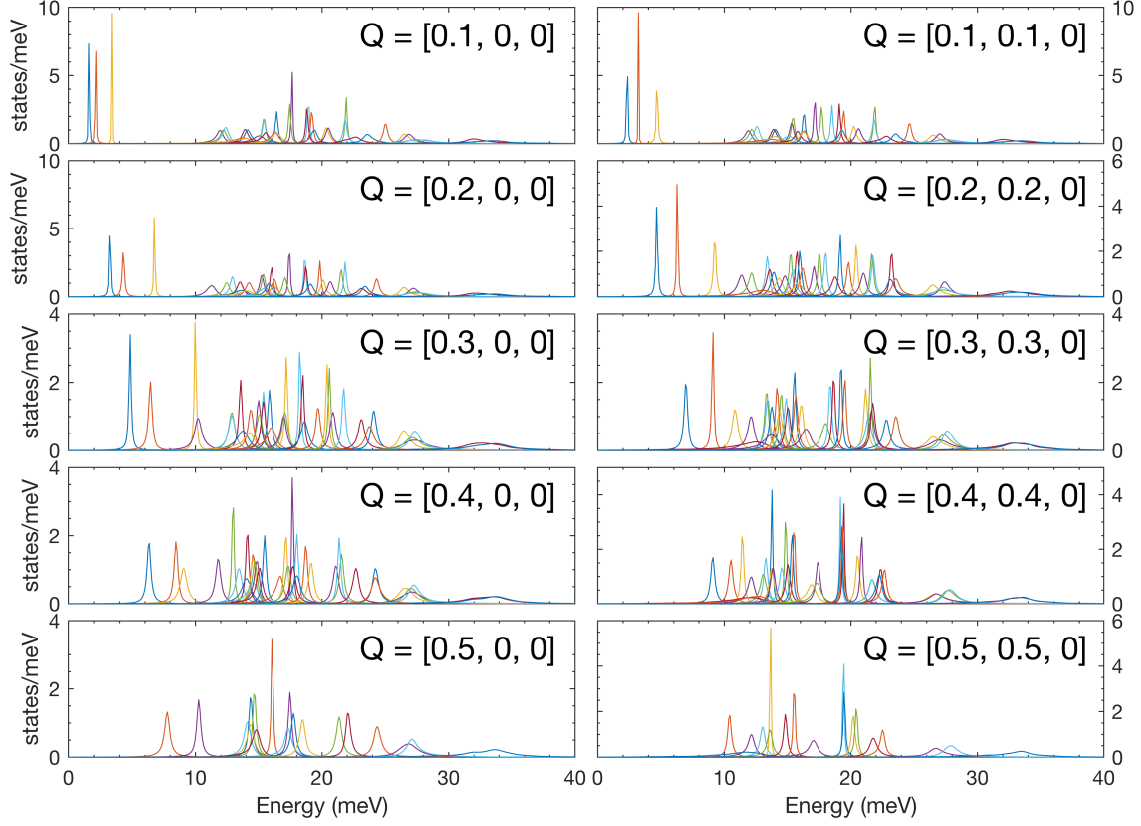


FIG. 12. **Calculated phonon spectrum function along  $[HH0]$  and  $[H00]$  directions in  $\text{FeGe}_2$  at 635 K.** The phonon spectrums along the two symmetry lines at 635K were calculated by *ab initio* stochastically initialized temperature-dependent effective potential method (s-TDEP) method. Colors represent different phonon branches.